INFLUENCE OF COMPRESSIVE STRENGTH AND WALL THICKNESS ON BEHAVIOR OF CONCRETE CYLINDRICAL HULLS UNDER HYDROSTATIC LOADING

N. D. Albertsen

Naval Civil Engineering Laboratory

Prepared for:

Naval Facilities Engineering Command

June 1973

Technical Report

R 790

Sponsored by

NAVAL FACILITIES ENGINEERING COMMAND

June 1973

NAVAL CIVIL ENGINEERING LABORATORY

Port Hueneme, California 93043

INFLUENCE OF COMPRESSIVE STRENGTH AND WALL THICKNESS ON BEHAVIOR OF CONCRETE CYLINDRICAL HULLS UNDER HYDROSTATIC LOADING

By

N. D. Albertsen

INFLUENCE OF COMPRESSIVE STRENGTH AND WALL THICKNESS ON BEHAVIOR OF CONCRETE CYLINDRICAL HULLS UNDER HYDROSTATIC LOADING

Technical Report R-790

3.1610-1

by

N. D. Albertsen

ABSTRACT

Sixteen unreinforced, cylindrical concrete hull models of 16-inch outside diameter were subjected to external hydrostatic loading to determine the effect of concrete strength and wall thickness on implosion and strain behavior. The test results showed that an increase in concrete strength of 70% produced an average increase in implosion pressure of 87%, while increases in hull wall thickness by factors of 2 and 6 produced increases in implosion pressure by factors of approximately 2 and 11, respectively. Changes in concrete strength had little effect on strain behavior; however, strain magnitudes generally increased with increasing wall thickness when comparisons were made at a constant percentage of P_{im}. Design recommendations are presented to aid in the design of cylindrical concrete hulls for underwater use.

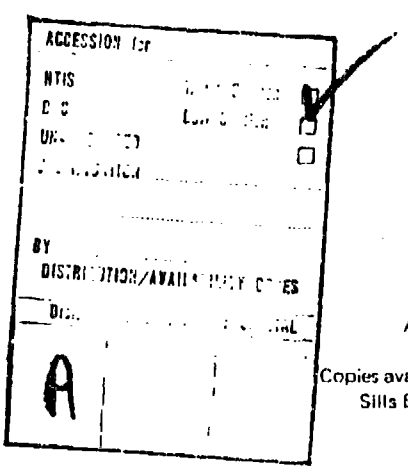

Unclassified

Security Classification

DOCUMENT CONTROL DATA - R & D

Security classification of title, body of abstract and indexing annotation must be entered when the overall report is classified

1 ORIGINATING ACTIVITY (Corporate author) Naval Civil Engineering Laboratory Port Hueneme, California 93043	2a. REPORT SECURITY CLASSIFICATION Unclassified 2b. GROUP

3 REPORT TITLE

INFLUENCE OF COMPRESSIVE STRENGTH AND WALL THICKNESS ON BEHAVIOR OF CONCRETE CYLINDRICAL HULLS UNDER HYDROSTATIC LOADING

4. DESCRIPTIVE NOTES (Type of report and inclusive dates)
Final; July 1970 – April 1972

5 AUTHOR(S) (First name, middle initial, last name)
N. D. Albertsen

6 REPORT DATE June 1973	7a. TOTAL NO OF PAGES 20 52	7b. NO OF REFS 11
8a CONTRACT OR GRANT NO. b. PROJECT NO 3.1610-1 c. d.	9a. ORIGINATOR'S REPORT NUMBER(S) TR-790 9b. OTHER REPORT NO(S) (Any other numbers that may be assigned this report)	

10 DISTRIBUTION STATEMENT
Approved for public release; distribution unlimited.

11. SUPPLEMENTARY NOTES	12. SPONSORING MILITARY ACTIVITY Naval Facilities Engineering Command Alexandria, VA 22332

13 ABSTRACT

Sixteen unreinforced, cylindrical concrete hull models of 16-inch outside diameter were subjected to external hydrostatic loading to determine the effect of concrete strength and wall thickness on implosion and strain behavior. The test results showed that an increase in concrete strength of 70% produced an average increase in implosion pressure of 87%, while increases in hull wall thickness by factors of 2 and 6 produced increases in implosion pressure by factors of approximately 2 and 11, respectively. Changes in concrete strength had little effect on strain behavior; however, strain magnitudes generally increased with increasing wall thickness when comparisons were made at a constant percentage of P_{im}. Design recommendations are presented to aid in the design of cylindrical concrete hulls for underwater use.

Details of illustrations in this document may be better studied on microfiche.

DD FORM 1 NOV 65 1473 (PAGE 1)

S/N 0101-807-6801

Unclassified

Security Classification

710

Unclassified

Security Classification

KEY WORDS	LINK A		LINK B		LINK C	
	ROLE	WT	ROLE	WT	ROLE	WT
Concrete cylindrical hulls						
Underwater applications						
Concrete strength						
Wall thickness						
Implosion behavior						
Strain behavior						
Hydrostatic loading						
Design guidelines						
Lame's equation						
Hemispherical end-closures						
Failure modes						
Compression-induced shear						
Buckling						
Bresse's equation						

DD FORM NOV. 1473 (BACK)

(PAGE 2)

Unclassified

Security Classification

CONTENTS

INTRODUCTION

Previous studies[1-8] conducted at the Naval Civil Engineering Laboratory (NCEL) have shown that concrete is an effective construction material for undersea pressure-resistant structures. Experiments on concrete cylindrical hulls[5,7] with 16-inch outside diameters, 2-inch-thick walls, and 8- to 128-inch lengths have established the influence of the length-to-outside-diameter, L/D_o, ratio and the end-closure stiffness on implosion pressure, strain magnitude, and strain distribution. Figure 1 shows that the thick wall theory based on Lamé's equation conservatively predicts implosion pressure for cylindrical concrete hulls with a wall-thickness-to-outside-diameter, t/D_o, ratio of 0.125 and L/D_o ratios from 0 to 8. The strain and implosion data for these hulls indicate that the effects of hemispherical concrete end-closures are minimal at a distance $\geq$ 1 diameter from the edge of the cylinder, and, thus, cylinders with L/D_o ratios greater than 2 can be considered to be infinitely long. Variations in end-closure stiffness did not cause a reduction in the implosion pressure of cylindrical concrete hulls below values predicted by Lamé's equation; however, rigid end-closures produced high shear strains near the closure which would be undesirable for structures subjected to long-term submergence.

The objective of this study was to determine experimentally the relationship between implosion pressure, concrete strength, wall thickness, strain distribution, and strain magnitude in cylindrical concrete hulls subjected to external hydrostatic loading.

Data from this experimental study were used to develop design guidelines so that safe and economical pressure-resistant cylindrical concrete structures can be designed for underwater applications.

EXPERIMENTAL PROGRAM

Experiment Design

Sixteen concrete cylindrical hulls having four different wall thicknesses and two concrete strengths were tested to implosion under short-term hydrostatic loading. The hulls had wall thicknesses of 1/2, 1,

2, and 3 inches (Figure 2) which correspond to t/D_o ratios of 0.0312, 0.0625, 0.1250, and 0.1875. All cylinders were 16 inches in outside diameter and 64 inches long; each had hemispherical concrete end-closures of the same wall thickness as the cylinder. Two hulls of each wall thickness were made of concrete with a uniaxial compressive strength, f'_c, of approximately 6,000 psi and two of approximately 10,000 psi. One hull of each concrete strength and wall thickness was instrumented with electrical resistance strain gages. A summary of the design information for the cylindrical hulls is given in Table 1.

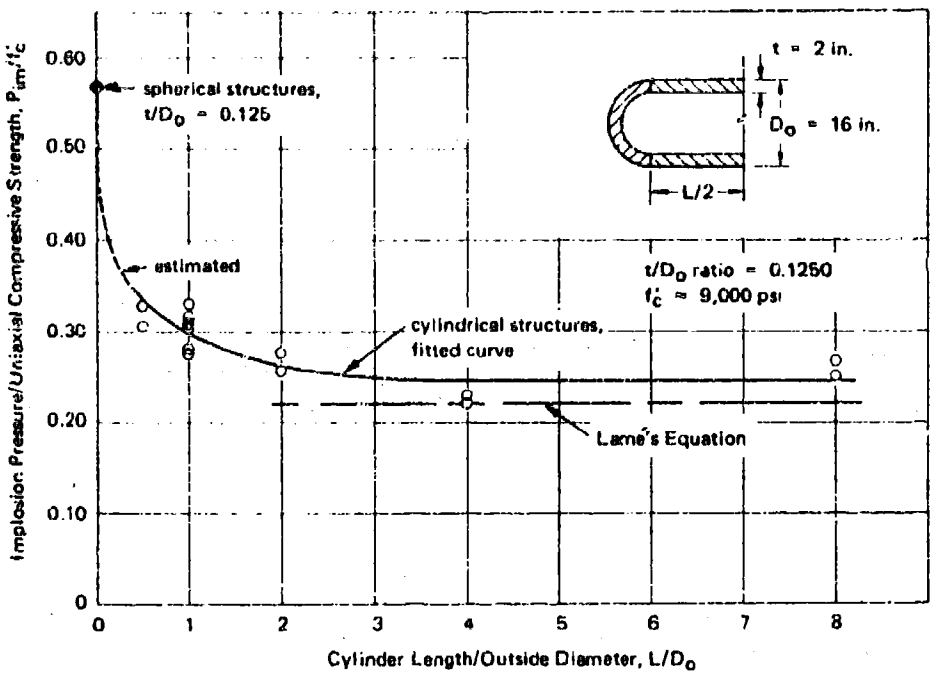

Figure 1. Analytical prediction of implosion pressure (after Reference 5).

Fabrication of Specimens

All cylinders and hemispherical end-closures were cast in rigid metal molds which had been machined to tolerances of ±1/32 inch. The cylinders and end-closures were made from a microconcrete mix consisting of type II portland cement, San Gabriel River Wash Aggregate, and freshwater. Concrete strengths of approximately 6,000 and 10,000 psi were produced by varying the water-to-cement ratio and the cure procedure. Table 2 gives the mix proportions and cure times, and Table 3 gives the aggregate proportions which remained the same for both mixes.

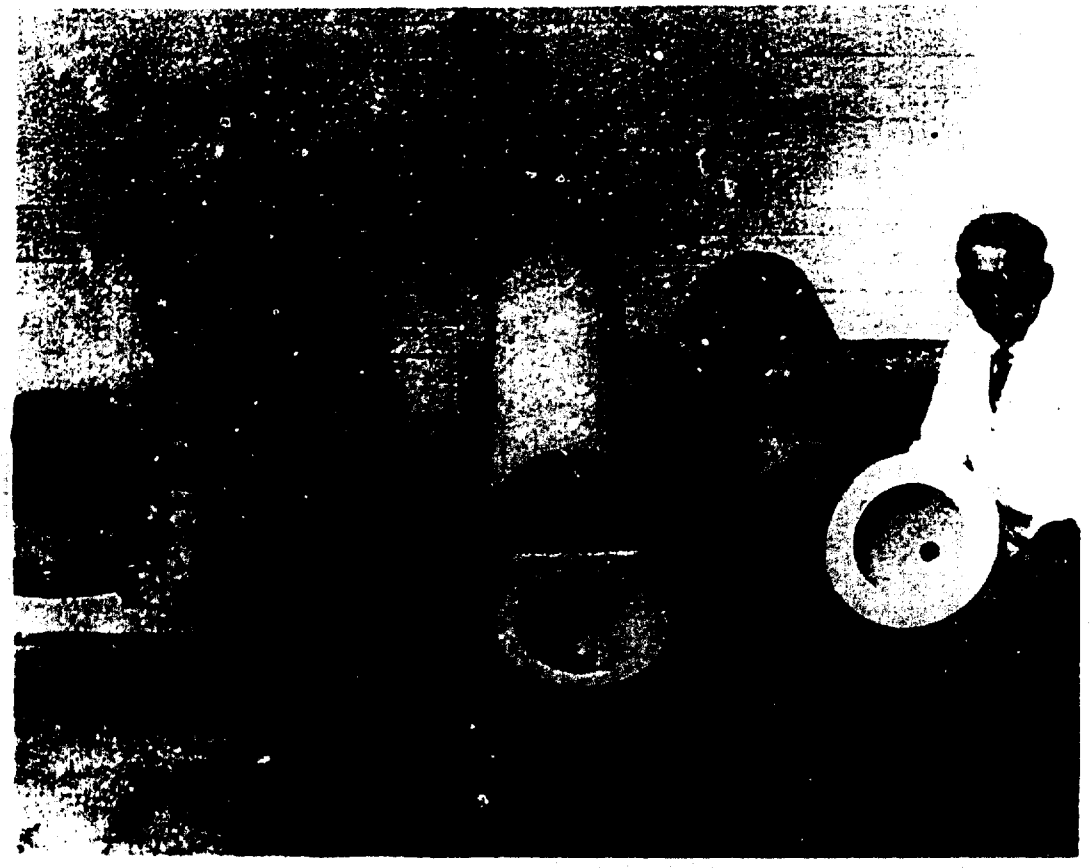

Figure 2. Cylindrical test specimens with wall thicknesses ranging from 1/2 inch to 3 inches.

After moist curing, the cylinders and end-closures were stored under room conditions while being prepared for test. Hull preparation began with a light sandblasting of surfaces to expose surface voids and to remove laitance. Small, shallow voids were filled with a cement-sand paste, while larger voids were filled with an epoxy adhesive. The mating surfaces of the cylinders and end-closures were ground flat by rotating them on a flat plate covered with No. 60 Silicon Carbide grit. Next the cylinders and hemispheres were waterproofed with a clear epoxy paint and bonded together with an epoxy adhesive. The final step in the specimen fabrication was to apply electrical resistance strain gages. Figure 3 shows a cross section of a fabricated cylindrical hull, and Figure 4 shows the strain gage layout for the hulls.

Test Procedure

The cylindrical hulls were tested in NCEL's 72-inch pressure vessel (Figure 5). The hulls were filled with water and vented to outside the pressure vessel. During a typical test, external pressure was applied to the hull at a

constant rate until implosion occurred. The pressurization rate was 20 psi/min for the 1/2-inch-thick hulls and 100 psi/min for the 1-, 2-, and 3-inch-thick hulls. At selected pressure intervals, the strain gages were interrogated and the change in volume of the specimen was recorded. Change in volume was measured by collecting the water displaced under load from the hull's interior.

Table 1. Description of Cylindrical Hulls

(All cylinders were 64 inches long and 16 inches in outside diameter.)

Cylinder Designation[a]	t/D_o Ratio	Wall Thickness (in.)	Nominal Uniaxial Compressive Strength of Concrete (psi)	Strain Gages on Hull[b]
1/2-10-G	0.0312	0.5	10,000	1 to 34
1/2-10-N			10,000	0
1/2-6-G			6,000	1 to 14
1/2-6-N			6,000	0
1-10-G	0.0625	1.0	10,000	1 to 34
1-10-N			10,000	0
1-6-G			6,000	1 to 14
1-6-N			6,000	0
2-10-G	0.1250	2.0	10,000	1 to 34
2-10-N			10,000	0
2-6-G			6,000	1 to 14
2-6-N			6,000	0
3-10-G	0.1875	3.0	10,000	1 to 34
3-10-N			10,000	0
3-6-G			6,000	1 to 14
3-6-N			6,000	0

[a] Designation system is: Wall thickness (inches) --Nominal concrete strength (ksi)— Gaged or Not gaged hull.

[b] See Figure 4 for location of gages.

Table 2. Mix Proportions and Cure Times

Approximate Uniaxial Compressive Strength of Mix (psi)	Water-to-Cement (by weight) Ratio	Aggregate-to-Cement (by weight) Ratio	Cure Time in 100% RH (days)	Approximate Age at Test (days)
10,000	0.56	3.30	90	120
6,000	0.65	3.30	7	28

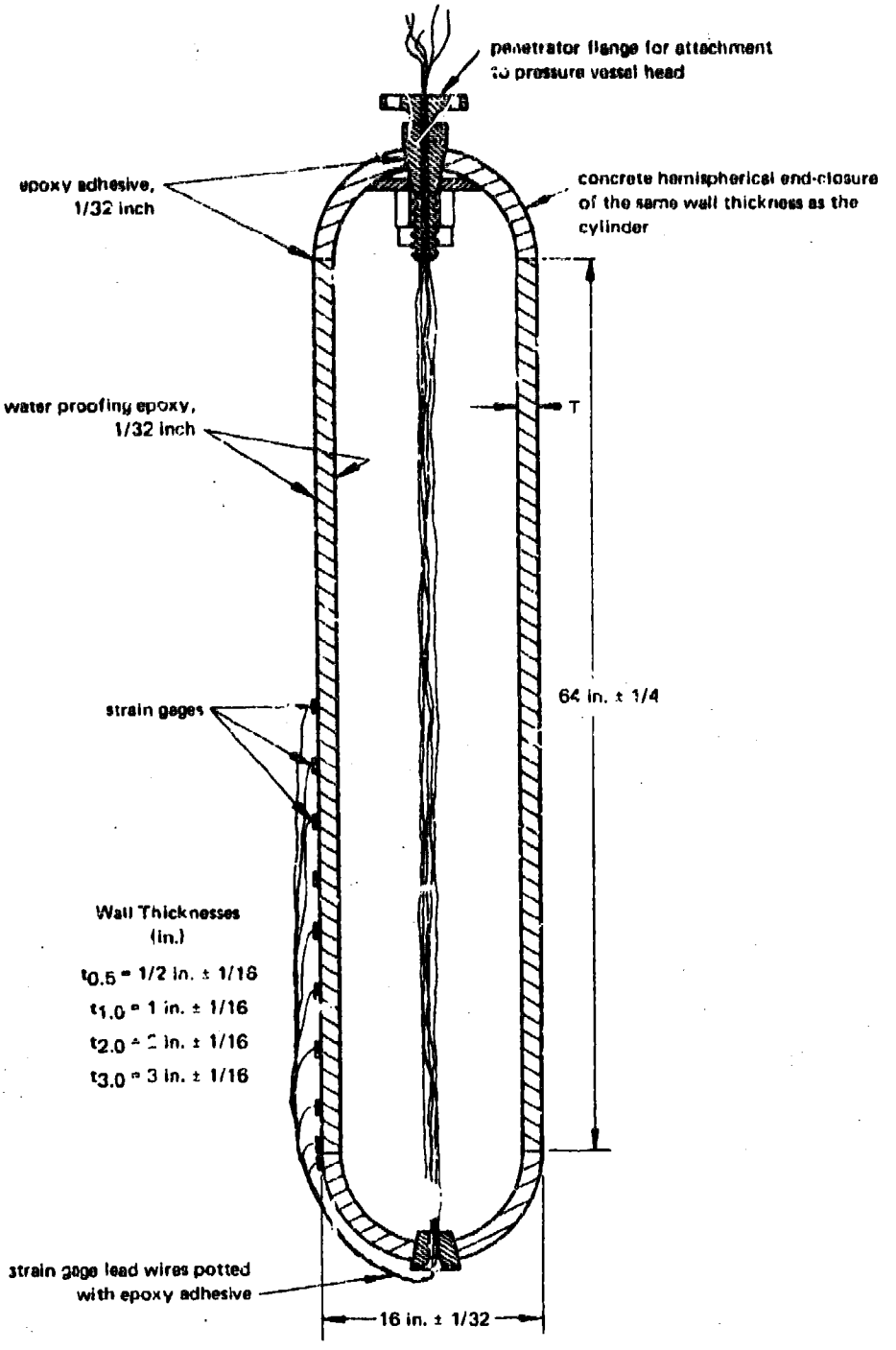

Figure 3. Cross-section of cylindrical hull with hemispherical end-closures.

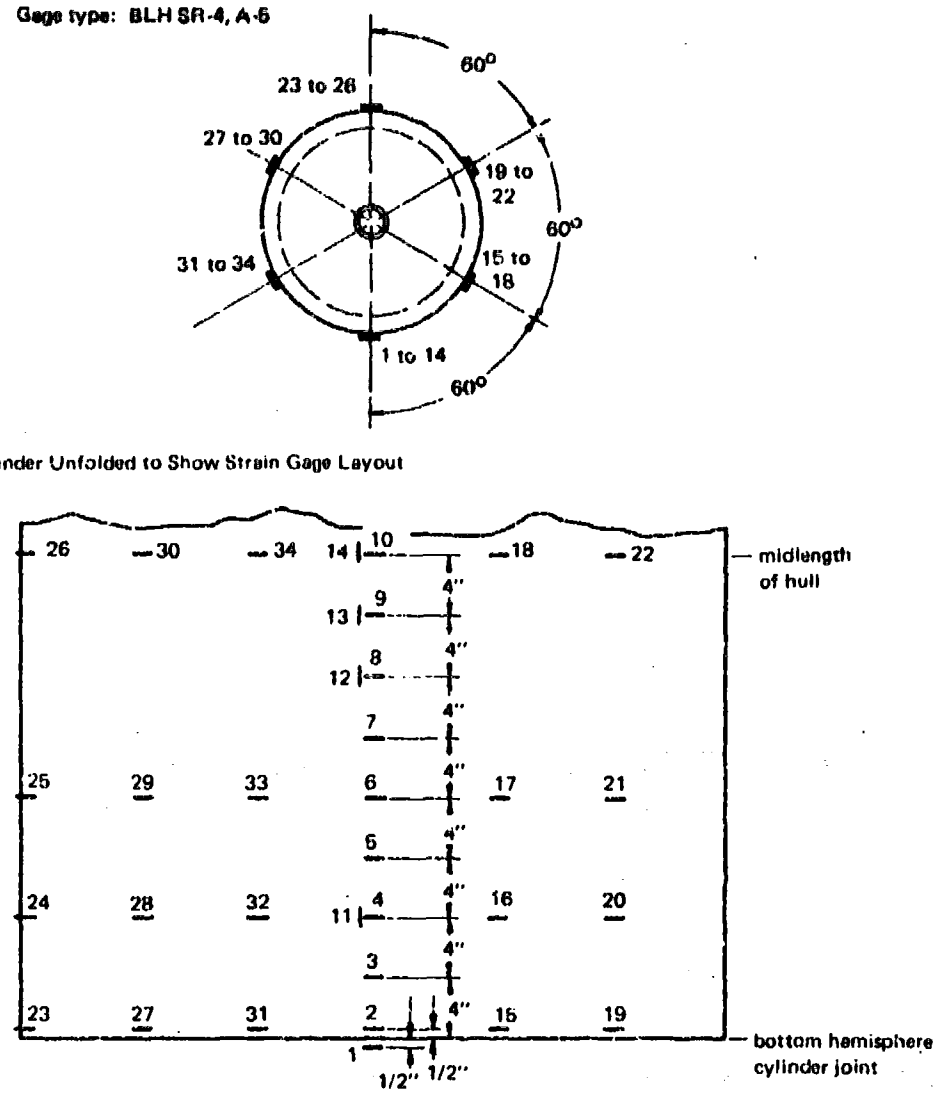

Figure 4. Strain gage layout for the cylindrical hulls.

Table 3. Aggregate Proportions

Sieve Size Designation		Percent Retained
Passing	Retained	
No. 4	No. 8	29.6
No. 8	No. 16	20.8
No. 16	No. 30	14.7
No. 30	No. 50	10.3
No. 50	No. 100	7.3
No. 100	pan	17.3

Figure 5 Cylindrical concrete hull prior to being lowered into the pressure vessel for test.

TEST RESULTS AND DISCUSSION

Mode of Failure

Inspection of the hulls after testing indicated that failure occurred, depending on wall thickness, either by compression-induced shear or by buckling. Hulls with 1-, 2-, or 3-inch-thick walls imploded when the concrete failed in the compressive-shear mode. The resulting shear plane could be easily identified by examining the specimens after test. A typical shear plane is shown in Figure 6. The shear planes were oriented parallel to the longitudinal axis of the cylinder and formed an angle of from 20 to 40 degrees with a tangent to the exterior surface. In most cases, the midlength of the shear plane was between 16 and 24 inches from the edge of the cylinder and coincided with the center of the implosion hole. This failure mode is representative of material failure.

Figure 6. Compressive shear failure of specimen 3-10-N.

The shear planes that were evident in the thicker hulls were completely absent from the 1/2-inch-thick hulls. These hulls shattered into many pieces at failure (Figure 7), which made it impossible to locate the initial point of failure. The mode of failure for these thin specimens appeared to be by buckling, because at failure the maximum wall stresses ranged from 53 to 62 percent of the uniaxial compressive strength of the concrete (Table 4).

Figure 7. Fragments of specimen 1/2-10-G.

Table 4 Implosion Test Results

Specimen Number	Wall Thickness[a] (in.)	Compressive Strength of Concrete,[b] f'_c (psi)	Implosion Pressure, P_{im} (psi)	$\frac{P_{im}}{f'_c}$	Calculated Interior Hoop Stress at Implosion, σ_{Hmax} (psi)	$\frac{\sigma_{Hmax}}{f'_c}$
1/2-10-N	1/2	10,700	376	0.035	6,210	0.58
1/2-10-G		10,900	349	0.032	5,765	0.53
1/2-6-N		5,420	203	0.037	3,355	0.62
1/2-6-G		5,760	214	0.037	3,535	0.61
1-10-N	1	10,700	1,110	0.104	9,470	0.88
1-10-G		10,480	1,103	0.105	9,410	0.90
1-6-G		6,620	547	0.083	4,665	0.70
1-6-N		5,920	530	0.090	4,520	0.76

(continued)

Table 4. Continued

Specimen Number	Wall Thickness[a] (in.)	Compressive Strength of Concrete,[b] f'_c (psi)	Implosion Pressure, P_{im} (psi)	$\frac{P_{im}}{f'_c}$	Calculated Interior Hoop Stress at Implosion, σ_{Hmax} (psi)	$\frac{\sigma_{Hmax}}{f'_c}$
2-10-G	2	9,840	2,335	0.237	10,670	1.08
2-10-N		9,950	2,455	0.247	11,220	1.13
2-6-N		6,080	1,387	0.228	6,340	1.04
2-6-G		6,060	1,447	0.238	6,615	1.09
3-10-G	3	10,350	3,755	0.363	12,315	1.19
3-10-N		10,800	4,107	0.380	13,470	1.25
3-6-N		7,000	2,405	0.344	7,890	1.13
3-6-G		6,200	1,980	0.319	6,495	1.05

[a] Wall thicknesses of 1/2, 1, 2, and 3 inches correspond to t/D_o ratios of 0.0312, 0.0625, 0.1250, and 0.1875, respectively.

[b] Average of six 3 x 6-inch control cylinders tested in uniaxial compression (see the Appendix).

No evidence was found in the debris from the tested specimens to indicate the presence of in-plane cracking. In-plane cracking is the development of cracks parallel to the maximum principal stresses (or in-the-plane of the wall) and has been found by other investigators working with concrete spherical[4] and cylindrical[5,11] hulls under biaxial stresses.

Implosion

Implosion performance was evaluated by comparing values for the ratio of implosion pressure to concrete strength, P_{im}/f'_c; the implosion test results are presented in Table 4. This ratio accounts for small variations in concrete strength. Figure 8 shows the best fit relationship between P_{im}/f'_c and t/D_o for the test results. The empirical equation which defines the best fit curve is:

$$\frac{P_{im}}{f'_c} = 2.05 \frac{t}{D_o} - 0.028 \qquad (1)$$

for $0.0312 \leq t/D_o \leq 0.1875$. Equation 1 can be used to predict the implosion pressure of cylindrical concrete hulls under hydrostatic loading.

The implosion pressure for concrete cylindrical hulls subjected to hydrostatic loading can be estimated by classical equations. Lame's equation can be used to estimate the implosion pressure of cylindrical hulls which fail

in the compressive shear mode, if failure is assumed to occur when the maximum principal stress reaches the uniaxial compressive strength of the concrete.[9] Lamé's equation is

$$P_{im} = f'_c \frac{r_o^2 - r_i^2}{2 r_o^2} \qquad (2)$$

where P_{im} = implosion pressure due to compressive shear failure (psi)

f'_c = uniaxial compressive strength of concrete (psi)

r_i = exterior radius of hull (in.)

r_o = interior radius of hull (in.)

The implosion pressure of cylindrical concrete hulls of finite length that fail by buckling can be estimated by Bresse's equation.[10] The equation is:

$$P_{cr} = \frac{2 E_s}{1 - \nu^2} \left(\frac{t}{D}\right)^3 \qquad (3)$$

where P_{cr} = implosion pressure due to buckling (psi)

E_s = secant modulus of elasticity to 0.5 f'_c (psi)

ν = Poisson's ratio at 0.5 f'_c

t = wall thickness of the hull (in.)

D = mean hull diameter (in.)

A graphical presentation of Equations 2 and 3 is also given in Figure 8.

Figure 8 shows that the 1/2- and 1-inch-thick hulls (t/D_o = 0.0312 and 0.0625) imploded at pressures lower than those predicted by Equation 2, while the 2- and 3-inch-thick hulls (t/D_o = 0.1250 and 0.1875) imploded at pressures higher than those predicted by Equation 2. For the thinner hulls, structural instability kept the concrete from developing its full compressive strength before buckling or premature compressive shear failure occurred. For the thicker hulls, the concrete in the walls was under a state of multi-axial stress which permitted the concrete to resist stresses greater than the uniaxial strength. At implosion, the 2- and 3-inch-thick hulls experienced stresses that *exceeded* f'_c by 4 to 25% (Table 4).

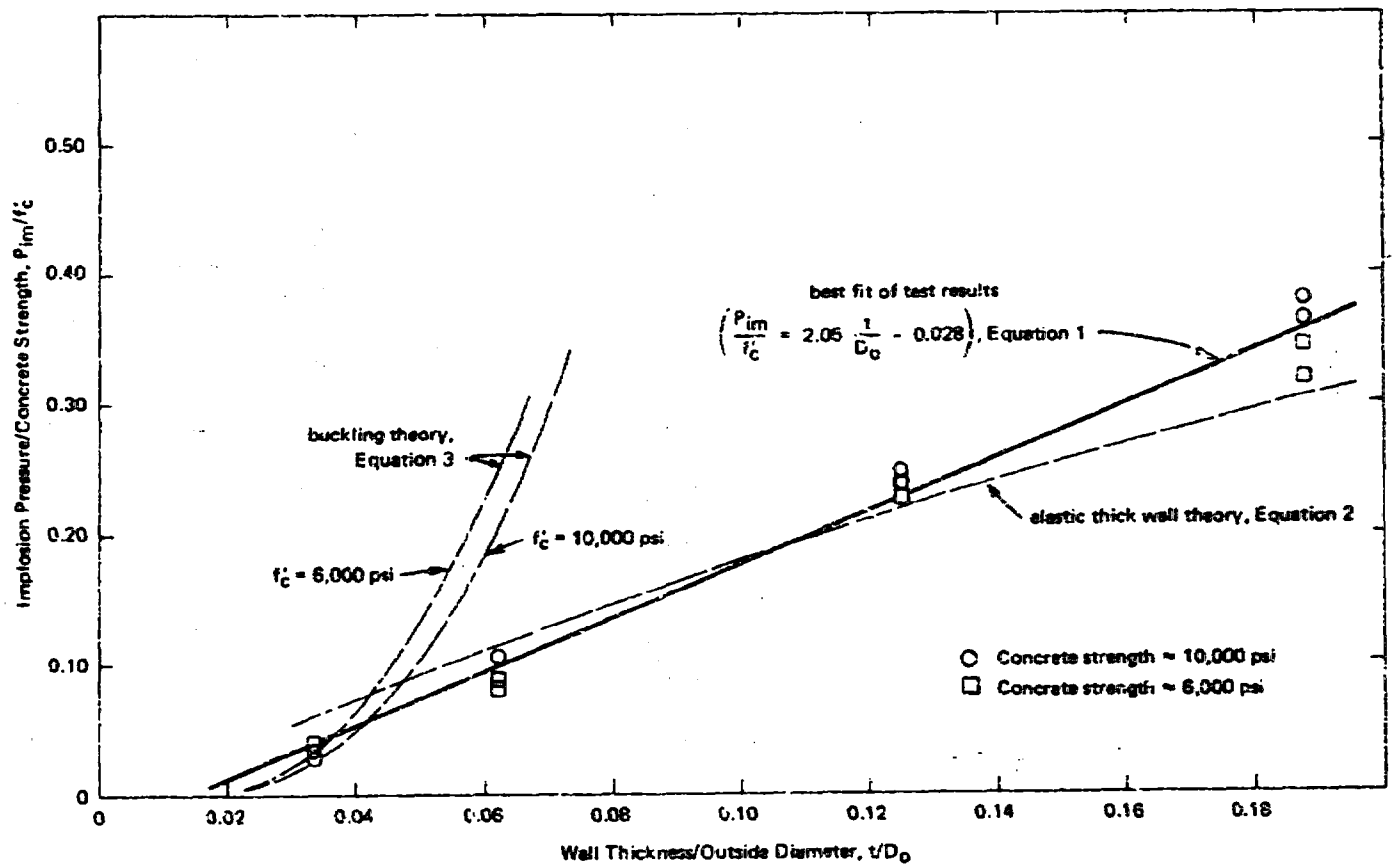

Figure 8. Comparison of implosion test results with elastic thick wall theory and buckling theory.

Strain

Figures 9 through 18 show the strain and radial displacement data for the instrumented hulls. These data helped to define the influence of wall thickness, concrete strength, and end-closure effects on the behavior of the hulls.

Figures 9 through 12 show the exterior hoop strain behavior for specimens of each wall thickness. These figures indicate that the hulls reacted to increasing hydrostatic pressure in approximately the same manner regardless of concrete strength. Within one outside diameter (16 inches) from the edge of the cylinder, large variations in strain magnitude were present; these variations in strain magnitude increased with increased pressure. Beyond 16 inches the strain magnitudes became somewhat uniform. This behavior was caused by the stiffness mismatch that existed between the stiff hemispherical end-closure and the more compliant cylinder; this is consistent with behavior observed in References 5 and 7.

The hoop strain data also show that as the hulls became thicker, the strain magnitude tended to become greater at a constant percentage of P_{im}. This behavior is reasonable because the concrete in the thicker walled hulls is subjected to higher triaxial loading conditions than the concrete in the thinner walled hulls. Table 5 shows that at 0.95 P_{im}, the theoretical radial stress component on a midwall element increased from 3 to 26% of the hoop stress component and from 6 to 41% of the axial stress component when the wall thickness was increased from 1/2 to 3 inches. It is known that concrete under a high triaxial loading state can sustain higher stresses and strains than concrete under a low triaxial (or biaxial/uniaxial) loading state.

Table 5. Theoretical Midwall Stresses at 0.95 P_{im}[a]

(All stresses are compressive.)

Wall Thickness, t (in.)	Applied External Pressure, P (psi)	Radial Stress, σ_R (psi)	Hoop Stress, σ_H (psi)	Axial Stress, σ_A (psi)	$\frac{\sigma_R}{\sigma_H}$	$\frac{\sigma_R}{\sigma_A}$
1/2	345	170	5,460	2,820	0.03	0.06
1	1,050	580	8,380	4,480	0.07	0.13
2	2,280	1,380	9,020	5,210	0.15	0.25
3	3,740	2,520	9,720	6,130	0.26	0.41

[a] P_{im} was 363, 1,105, 2,400, and 3,940 psi, respectively, for the 1/2-, 1-, 2-, and 3-inch-thick hulls.

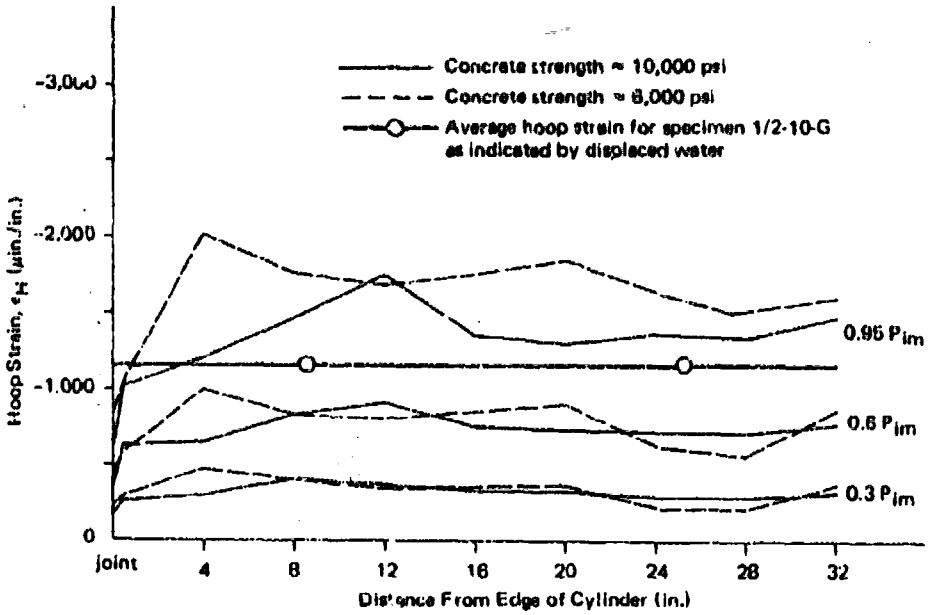

Figure 9. Exterior hoop strain for specimens 1/2-10-G and 1/2-6-G.

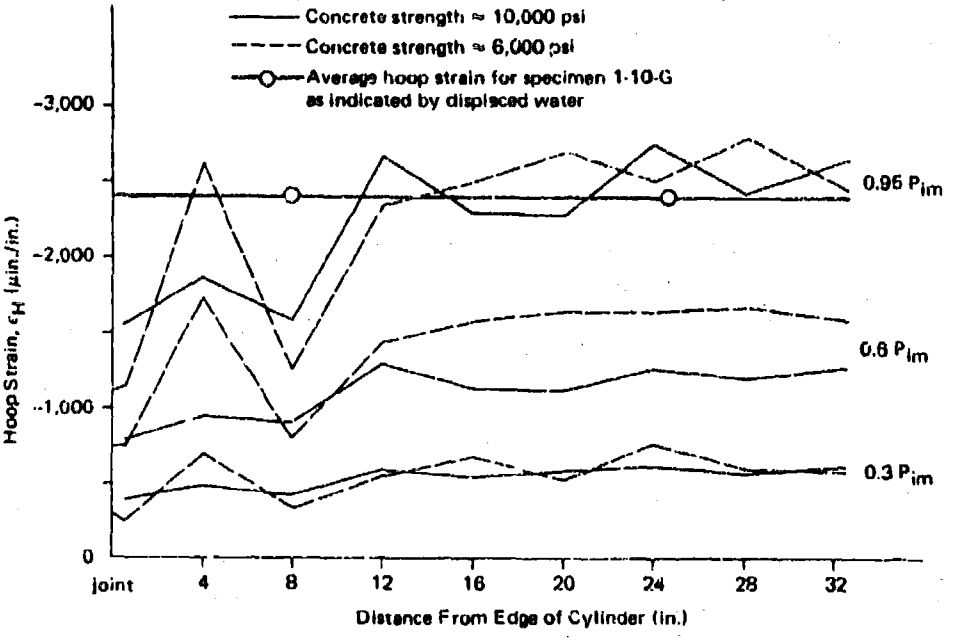

Figure 10. Exterior hoop strain for specimens 1-10-G and 1-6-G.

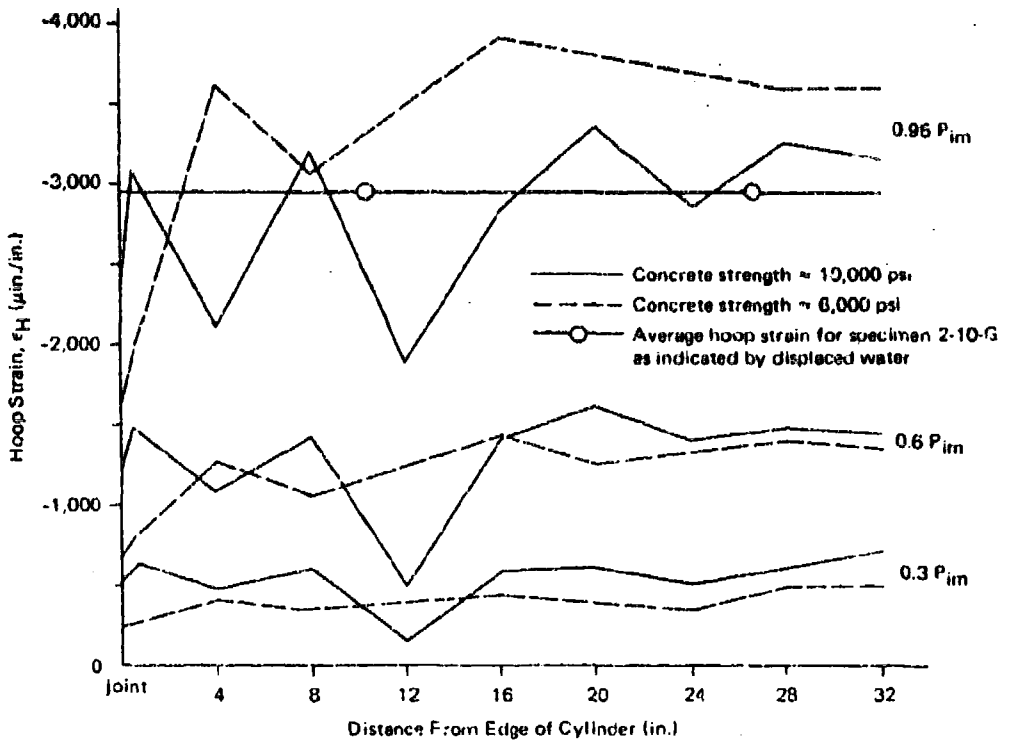

Figure 11. Exterior hoop strain for specimens 2-10-G and 2-6-G.

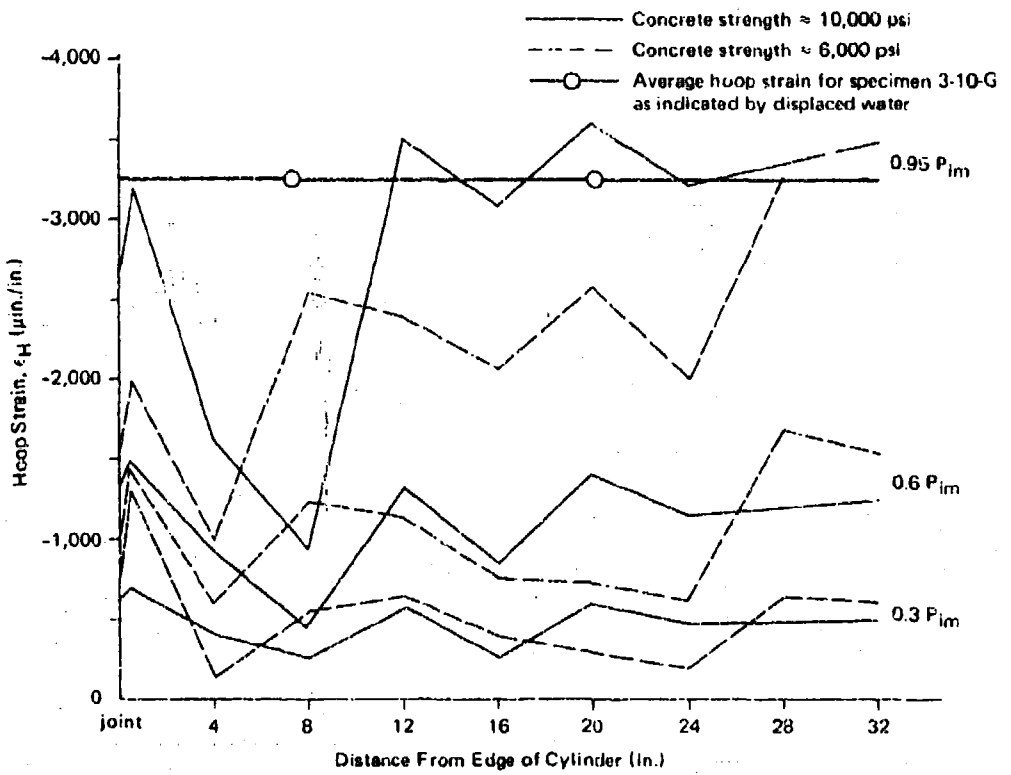

Figure 12. Exterior hoop strain for specimens 3-10-G and 3-6-G.

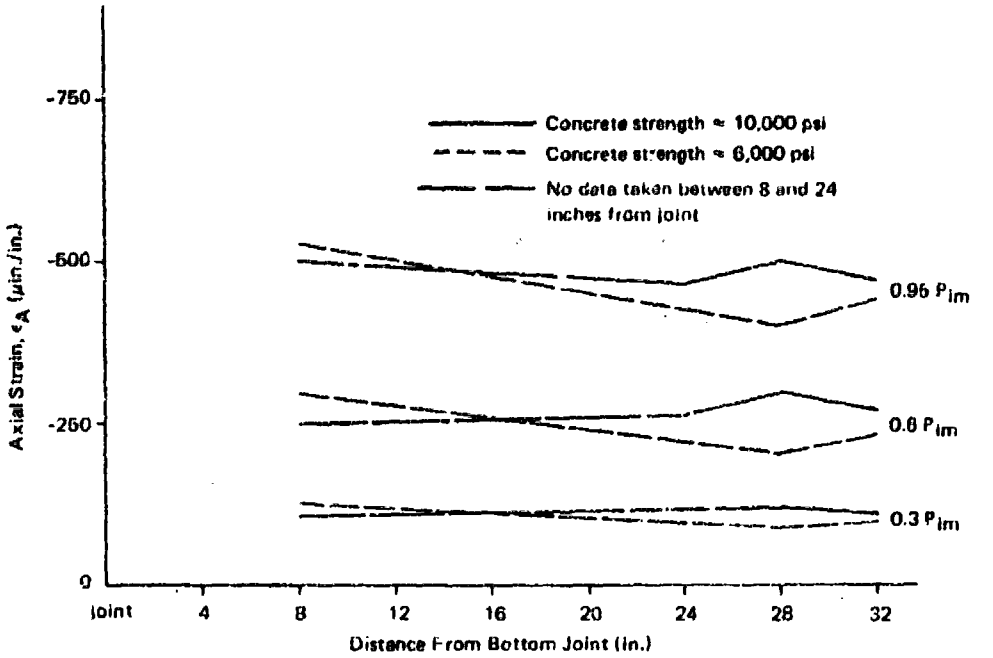

Figure 13. Exterior axial strain for specimens 1/2-10-G and 1/2-6-G.

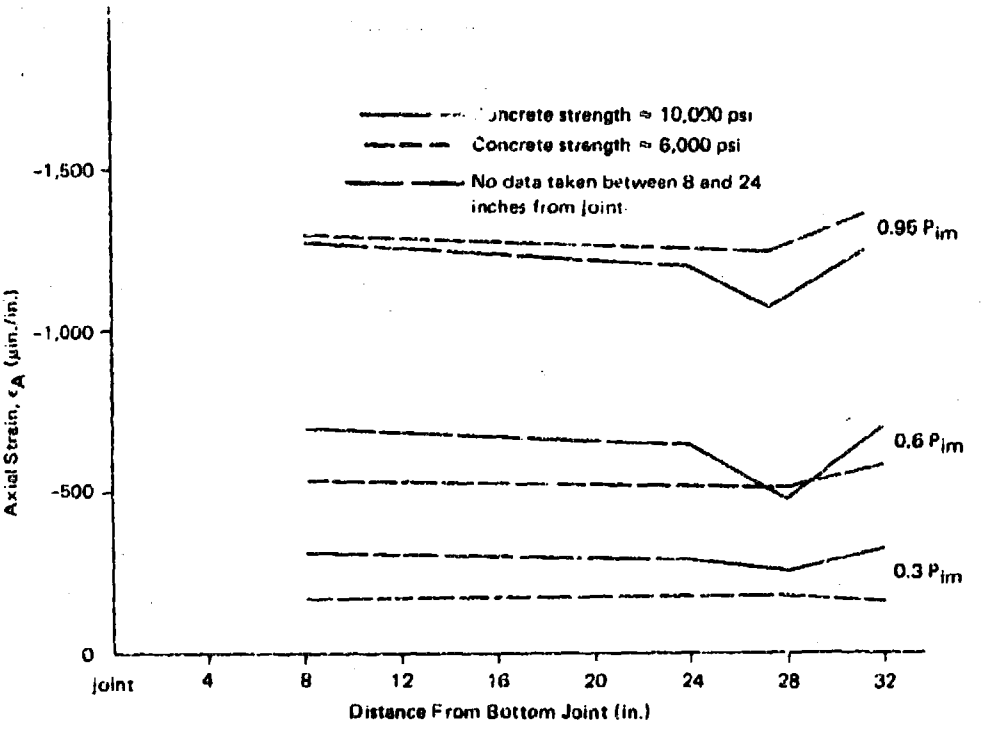

Figure 14. Exterior axial strain for specimens 2-10-G and 2-6-G.

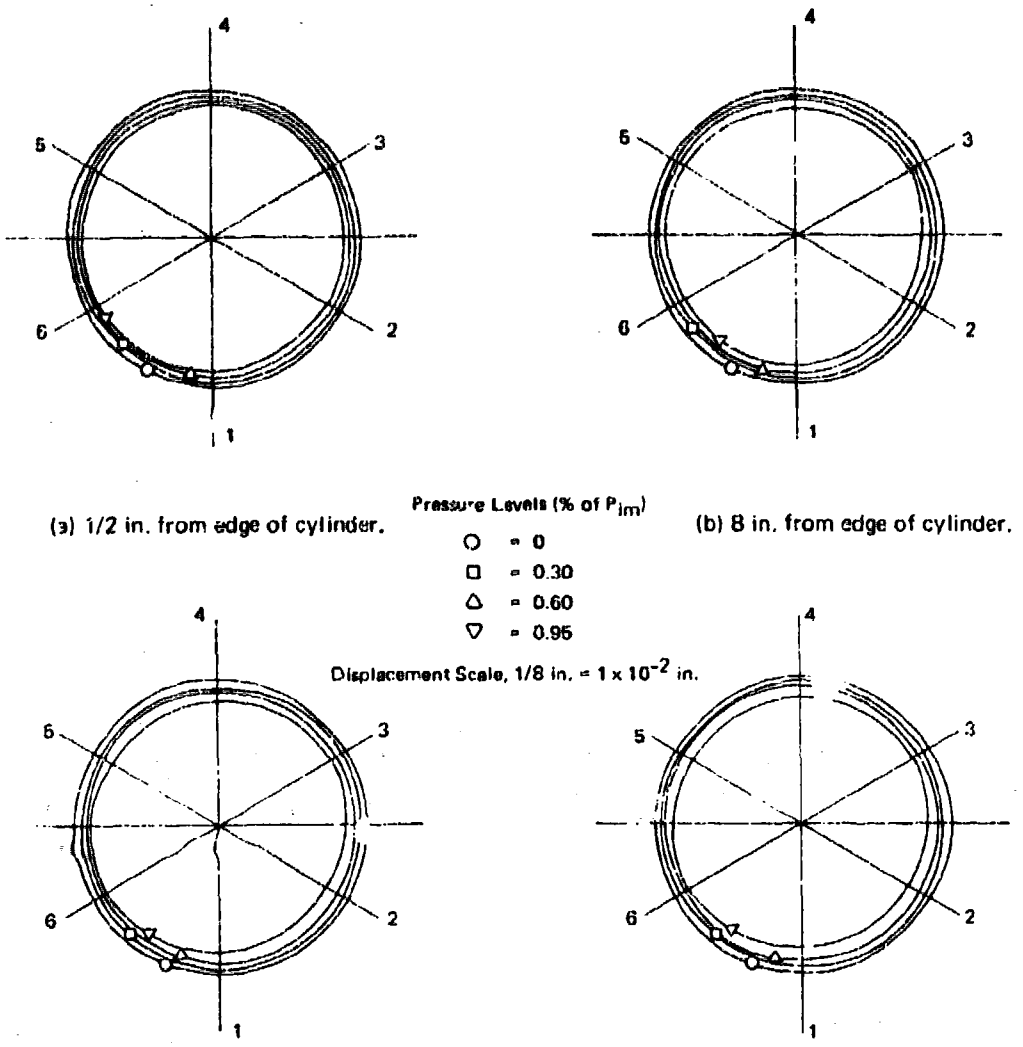

(a) 1/2 in. from edge of cylinder.

(b) 8 in. from edge of cylinder.

(c) 16 in. from edge of cylinder.

(d) 32 in. from edge of cylinder.

Figure 15. Radial displacement of the exterior surface of specimen 1/2-10-G.

The change-in-volume data were converted to average exterior hoop strain by the thick wall theory. These calculated average values for hoop strain are plotted in Figures 9 through 12 at 0.95 P_{im} and serve as a check on the strain gage data.

Figures 13 and 14 show the axial strain behavior of 1/2- and 2-inch-thick cylinders, respectively. These figures are typical for the behavior of all the instrumented cylinders. In general, the axial strain at 8 inches from the edge of the cylinder was the same as that near the cylinder's midlength. No distinct trends in axial strain behavior were found that could be attributed to variations in concrete strength.

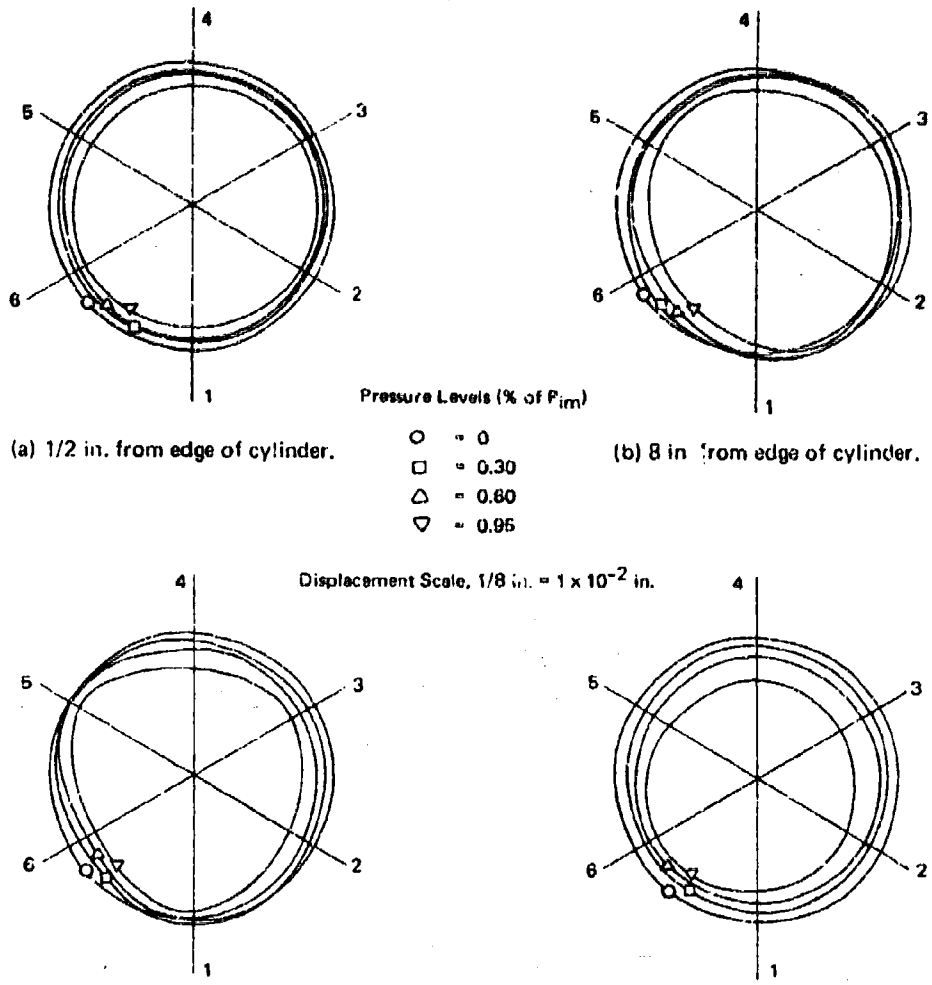

(a) 1/2 in. from edge of cylinder.

(b) 8 in from edge of cylinder.

(c) 16 in. from edge of cylinder.

(d) 32 in. from edge of cylinder

Figure 16. Radial displacement of the exterior surface of specimen 1-10-G.

Figures 15 through 18 show the radial displacement* of the exterior surface for the cylindrical hulls. These figures reveal some interesting patterns of behavior. At 1/2 and 32 inches from the edge of the cylinder, all specimens remained quite circular at all levels of pressure. At 8 and 16 inches from the edge, the 1- and 3-inch-thick specimens showed marked deviations from axial symmetry and large amounts of out-of-roundness under load. The probable cause for the deviations from symmetry and roundness is the presence of initial out-of-roundness in the specimens combined with the influence of the stiffness mismatch between the hemispherical end-closure and the cylinder.

* Radial displacement is the product of hoop strain and radius to the surface of interest.

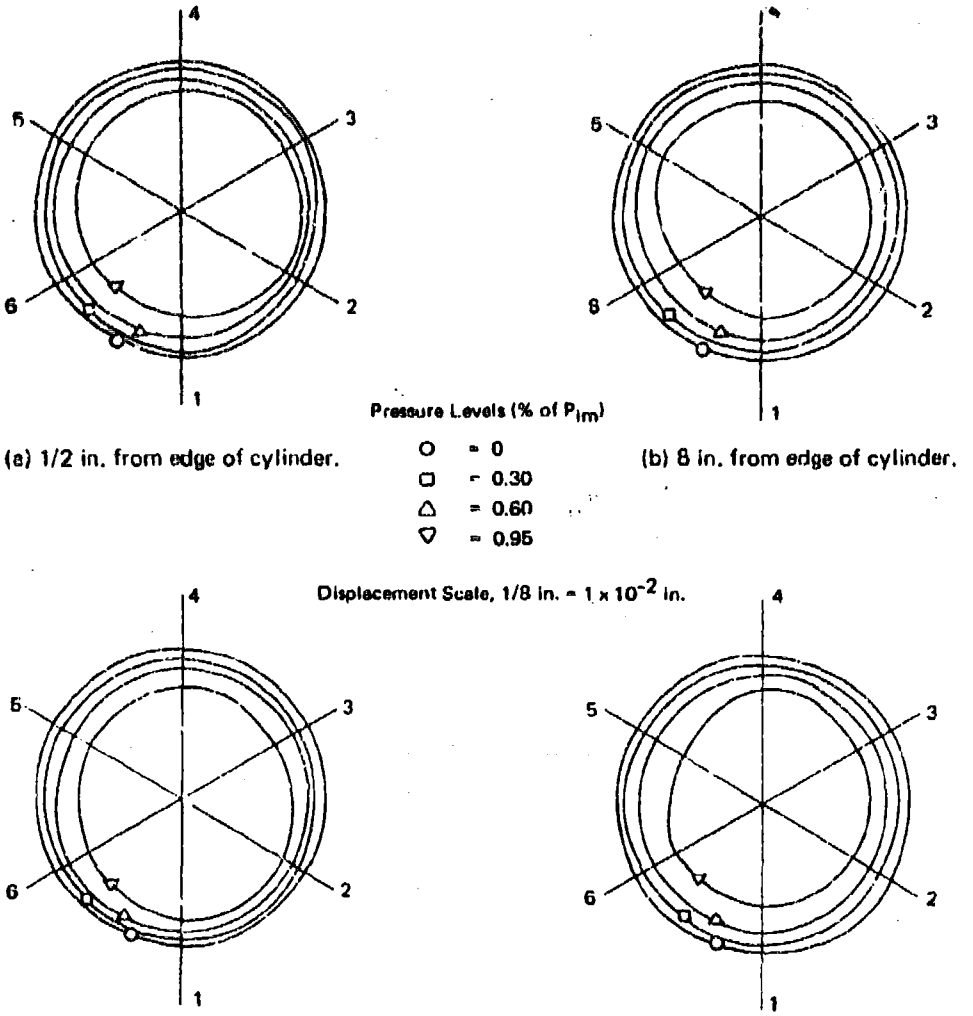

(a) 1/2 in. from edge of cylinder.

(b) 8 in. from edge of cylinder.

(c) 16 in. from edge of cylinder.

(d) 32 in. from edge of cylinder.

Figure 17. Radial displacement of the exterior surface of specimen 2-10-G.

DESIGN PROBLEM

Design a cylindrical concrete hull of 25-foot inside diameter, 100-foot length (cylinder portion only) and 100,000-pound positive buoyancy for long-term operation at a depth of 1,000 feet. Assume the use of hemispherical end-closures of the same wall thickness as the cylinder and concrete of 7,000-psi uniaxial compressive strength.

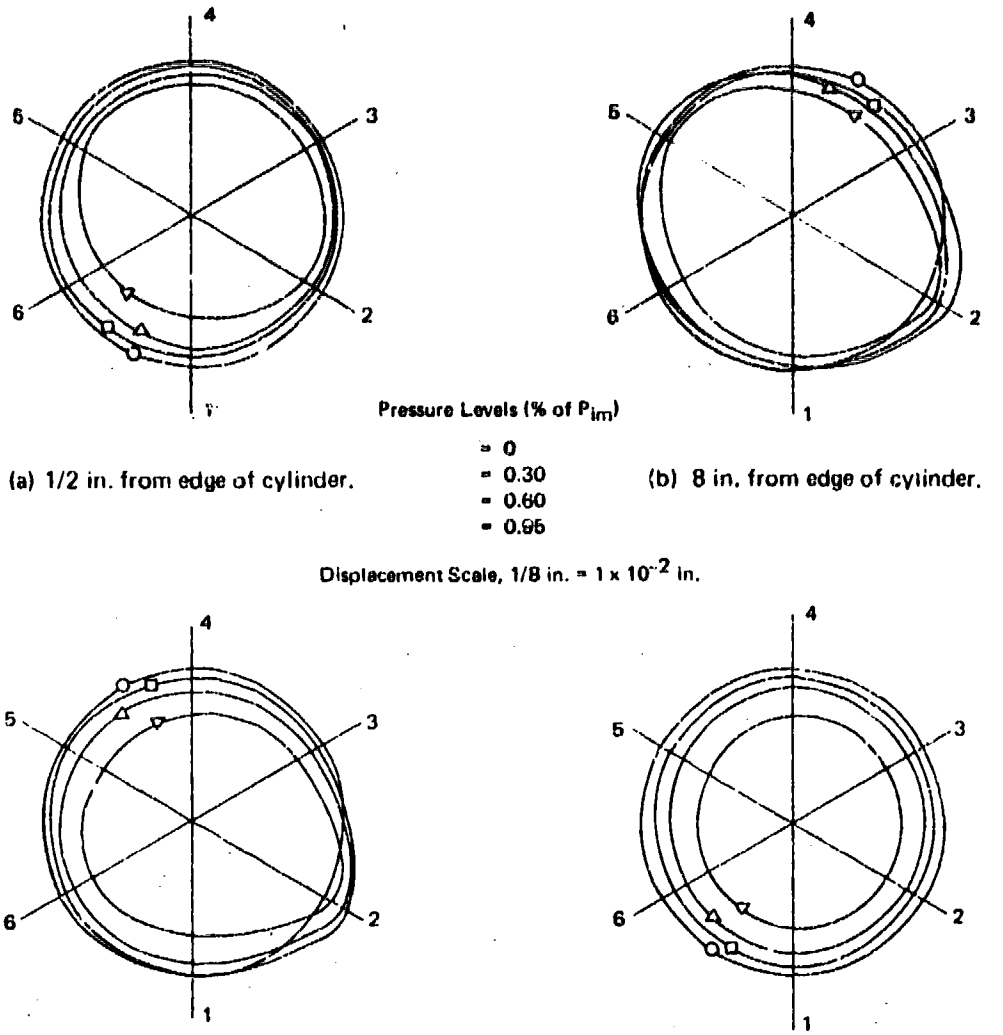

(a) 1/2 in. from edge of cylinder.

(b) 8 in. from edge of cylinder.

(c) 16 in. from edge of cylinder

(d) 32 in. from edge of cylinder.

Figure 18. Radial displacement of the exterior surface of specimen 3-10-G.

Because a buoyancy requirement is part of the example problem, the first step is to determine *cylinder wall thickness* based on buoyancy.

$$\text{(a) Displacement of hull} = 64\left(\frac{\pi}{6} D_o^3 + \frac{100\pi}{4} D_o^2\right)$$

$$= 33.51\, D_o^3 + 5{,}027\, D_o^2$$

(b) Weight of hull $= 150\left[\frac{\pi}{6}(D_o^3 - 25^3) + \frac{100\pi}{4}(D_o^2 - 25^2)\right]$

$= 78.54\,D_o^3 + 11{,}780\,D_o^2 - 8{,}590{,}000$

(c) Displacement - Weight = Buoyancy

(1) $(33.51\,D_o^3 + 5{,}027\,D_o^2) - (78.54\,D_o^3 + 11{,}780\,D_o^2 - 8{,}590{,}000)$

$= 100{,}000$

(2) $45.03\,D_o^3 + 6{,}753\,D_o^2 = 8{,}490{,}000$

(3) $D_o = 32.17$ ft

(d) Wall thickness, $t = \frac{D_o - D_i}{2}$

$= \frac{32.17 - 25.00}{2}$

$= 3.58$ ft

Next, it is necessary to check the design to be sure that there is a *safety factor* of at least 3 on the structure as it may be manned and used for long-term operations.

(a) $P_{im} = f'_c\left(2.05\,\frac{t}{D_o} - 0.028\right)$ (1)

$= 7 \times 10^3\left(2.05\,\frac{3.58}{32.17} - 0.028\right)$

$= 1{,}397$ psi

(b) Convert 1,397 psi to depth of water in feet:

Implosion Depth $= 1{,}397 \times 2.24$

$= 3{,}130$ ft

$$\text{(c) Safety Factor} = \frac{\text{Implosion Depth}}{\text{Operating Depth}}$$

$$= 3{,}130/1{,}000$$

$$= 3.13$$

Since the safety factor is greater than 3.0, the wall thickness derived through buoyancy considerations is, therefore, satisfactory. If the safety factor had turned out to be less than 3.0, then a concrete mix with a compressive strength greater than the specified 7,000 psi would have been required.

If the structure's buoyancy is not of major concern, Figure 19 can be used to quickly determine the cylinder wall thickness needed for a given depth and factor of safety. To solve the example problem using Figure 19 as the design guide, the following steps are required.

(a) Convert operating depth to pressure in psi:

$$\text{Pressure, } P = 1{,}000 \text{ ft} \times 0.446 = 446 \text{ psi}$$

(b) Calculate P/f'_c:

$$P/f'_c = \frac{446}{1{,}000} = 0.064$$

(c) Enter Figure 19 at $P/f'_c = 0.064$ and read across until the 3.0 factor of safety curve is intersected. Read out $t/D_o = 0.108$

(d) Since $t = (D_o - D_i)/2$, $t = 0.108\, D_o$, and $D_i = 25.00$ ft, then

$$D_o = 31.89 \text{ ft}$$

$$t = 3.44 \text{ ft}$$

Note that the wall thickness obtained using Figure 19 is slightly less than that obtained using Equation 3 and buoyancy considerations. This is because depth controlled the design of Figure 19; the result is a structure that has approximately 150,000 pounds more buoyancy than the 100,000 pounds specified in the example problem.

The final design of cylindrical concrete hulls for use in the ocean would have to include steel reinforcement to resist handling loads; such design measures can be accomplished with conventional reinforced/prestressed design techniques and are not included herein.

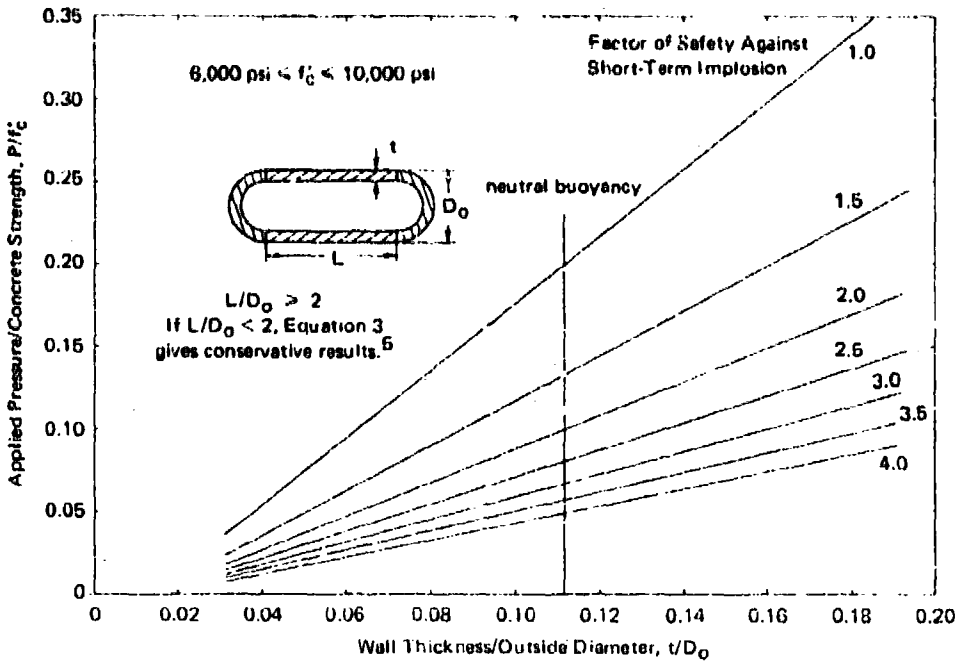

Figure 19. Design guideline for cylindrical concrete hulls with hemispherical end-closures (based on Equation 1).

FINDINGS

1. The implosion pressures for the concrete cylindrical hulls showed a direct relationship to increases in concrete strength from 6,000 to 10,000 psi and to increases in the ratio of wall thickness to outside diameter for values from 0.0312 to 0.1875. A linear empirical equation, Equation 1, was developed to predict the implosion pressures.

2. Implosion pressures ranged from 208 psi for the 1/2-inch-thick hulls of 6,000-psi concrete strength to 3,930 psi for the 3-inch-thick hulls of 10,000-psi concrete strength.

3. Two modes of failure for the hulls were observed: the 1/2-inch-thick hulls (t/D_o = 0.0312) failed by buckling, while the 1-, 2-, and 3-inch-thick hulls (t/D_o = 0.0625, 0.1250, and 0.1875) failed by compression shear type material failure.

4. Strain data showed that end-closure effects were minimal beyond one outside diameter from the end-closure-to-cylinder joint.

CONCLUSIONS

This study on the influence of concrete strength and wall thickness and previous studies on the influence of cylinder length and end-closure stiffness have demonstrated that concrete is a predictable material for pressure-resistant cylindrical structures. It is estimated that buoyant, cylindrical concrete structures will have applications to the ocean depth of 1,500 feet.

RECOMMENDATIONS

1. It is recommended that Equation 1 or Figure 19 be used as a guideline for the design of cylindrical concrete hulls for use under the sea.

$$P_{im} = f'_c\left(2.05\ \frac{t}{D_o} - 0.028\right) \qquad (1)$$

where P_{im} = implosion pressure (psi)

f'_c = uniaxial compressive strength of concrete (psi)

t = wall thickness (ft)

D_o = outside diameter (ft)

2. It is recommended that the region between the end-closure-to-cylinder joint and one outside diameter from the joint not be used for penetrations in concrete cylindrical hulls if alternate locations are available. If this location is used for a penetration, then an appropriate increase in the factor of safety is recommended.*

ACKNOWLEDGMENTS

The author wishes to thank Mr. Harvey Haynes of the Ocean Structures Division for his constant interest, encouragement and many helpful suggestions. He also wishes to thank Mr. Philip Zubiate whose special efforts in the fabrication of the test specimens allowed the timely completion of the work.

* The effect of penetrations in cylindrical hulls is under study.

Appendix

CONTROL CYLINDER DATA

The test results from the 3 x 6-inch control cylinders for the cylindrical hulls are presented in Table A-1. The nominal 10,000-psi concrete strength mix produced average values for f'_c, E_s, and ν of 10,460 psi, 3.56×10^6 psi, and 0.19, respectively; the nominal 6,000-psi concrete strength mix produced average values of 6,130 psi, 2.68×10^6 psi, and 0.16, respectively, for the same three parameters. All hemispherical end-closures were made from a high-strength mix which had average values of 8,840 psi, 3.18×10^6 psi, and 0.17, respectively.

Table A-1. Test Results for 3 x 6-Inch Control Cylinders

Specimen Designation	Compressive Strength of Concrete, f'_c (psi)	Secant Modulus of Elasticity,[a] E_s (psi x 10^6)	Poisson's Ratio,[b] ν	Age at Test (days)
1/2-10-N	10,700	3.47	0.18	101
1/2-10-G	10,900	3.85	0.18	124
1/2-6-N	5,420	2.58	0.18	16
1/2-6-G	5,760	2.29	0.16	32
1-10-N	10,700	3.72	0.20	117
1-10-G	10,480	3.55	0.20	118
1-6-G	6,620	2.67	0.16	28
1-6-N	5,920	2.70	0.17	27
2-10-G	9,840	3.58	0.18	118
2-10-N	9,950	3.36	0.19	124
2-6-N	6,080	2.91	0.15	23
2-6-G	6,060	2.67	0.12	24
3-10-G	10,350	3.59	0.22	119
3-10-N	10,800	3.40	0.14	119
3-6-N	7,000	2.80	0.15	27
3-6-G	6,200	2.68	0.21	27

[a] Average of two 3 x 6-inch control cylinders to 0.5 f'_c.

[b] Average of two 3 x 6-inch control cylinders.

REFERENCES

1. Naval Civil Engineering Laboratory. Technical Report R-517: Behavior of spherical concrete hulls under hydrostatic loading, pt. 1. Exploratory investigation, by J. D. Stachiw and K. O. Gray. Port Hueneme, Calif., Mar. 1967. (AD 649290)

2. _____. Technical Report R-547: Behavior of spherical concrete hulls under hydrostatic loading, pt. 2. Effect of penetrations, by J. D. Stachiw. Port Hueneme, Calif., Oct. 1967. (AD 661187)

3. _____. Technical Report R-588: Behavior of spherical concrete hulls under hydrostatic loading, pt. 3. Relationship between thickness-to-diameter ratio and critical pressures, strains and water penetration rates, by J. D. Stachiw and K. Mack. Port Hueneme, Calif., June 1968. (AD 835492L)

4. _____. Technical Report R-679: Failure of thick-walled concrete spheres subject to hydrostatic loading, by H. H. Haynes and R. A. Hoofnagle. Port Hueneme Calif., May 1970. (AD 708011)

5. _____. Technical Report R-696. Influence of length-to-diameter ratio on behavior of concrete cylindrical hulls under hydrostatic loading, by H. H. Haynes and R. J. Ross. Port Hueneme, Calif., Sept. 1970. (AD 713088)

6. _____. Technical Report R-735: Influence of stiff equatorial rings on concrete spherical hulls subjected to hydrostatic loading, by L. F. Kahn and J. D. Stachiw. Port Hueneme, Calif., Aug. 1971. (AD 731352)

7. _____. Technical Report R-740: Influence of end-closure stiffness on behavior of concrete cylindrical hulls subjected to hydrostatic loading, by L. F. Kahn. Port Hueneme, Calif., Oct. 1971. (AD 732363)

8. _____. Technical Report R-774. Behavior of 66-inch concrete spheres under short and long term hydrostatic loading, by H. H. Haynes and L. F. Kahn. Port Hueneme, Calif., Sept. 1972. (AD 748584)

9. F. L. Singer. Strength of materials, 2nd ed. New York, Harper and Row, 1962, pp. 504-508.

10. S. Timoshenko. Theory of elastic stability, 2nd ed. New York, McGraw-Hill, 1961, pp. 289-293.

11. I. Rosenthal and J. Glucklich. "Strength of plain concrete under biaxial stress," American Concrete Institute, Journal, Proceedings, vol. 67, no. 11, Nov. 1970, pp. 903-914.

LIST OF SYMBOLS

D	Mean cylinder diameter (in.)
D_i	Inside diameter of cylinder (in.)
D_o	Outside diameter of cylinder (in.)
E_s	Secant modulus for the concrete to 0.5 f'_c (psi)
f'_c	Uniaxial compressive concrete strength (psi)
L	Length of cylinder (in.)
P	Applied pressure
P_{cr}	Implosion pressure due to buckling failure (psi)
P_{im}	Implosion pressure due to compressive shear failure (psi)
r_i	Interior radius of cylinder (in.)
r_o	Exterior radius of cylinder (in.)
t	Thickness of cylinder wall (in.)
ϵ_A	Axial strain (in./in.)
ϵ_H	Hoop strain (in./in.)
ν	Poisson's ratio
σ_A	Axial stress (psi)
σ_H	Hoop stress (psi)
σ_{Hmax}	Interior hoop stress at implosion
σ_R	Radial stress (psi)